Appl Biochem Biotechnol (2010) 160:879–890
DOI 10.1007/s12010-009-8666-0

Characterization of a Neutral and Thermostable Glucoamylase from the Thermophilic Mold *Thermomucor indicae-seudaticae*: Activity, Stability, and Structural Correlation

Pardeep Kumar · Asimul Islam · Faizan Ahmad · T. Satyanarayana

Received: 30 October 2008 / Accepted: 4 May 2009 /
Published online: 30 May 2009

Abstract Glucoamylase from the thermophilic mold *Thermomucor indicae-seudaticae* was purified by anion exchange and gel filtration chromatographic techniques using a fast protein liquid chromatographic system. The structure and thermal stability of this unique 'thermostable and neutral glucoamylase' were analyzed by circular dichroism (CD). *T. indicae-seudaticae* glucoamylase (TGA) contained typical aromatic amino acid (tryptophan/tyrosine) fingerprints in its tertiary structure. Analysis of the far-UV CD spectrum at pH 7.0 and 25 °C revealed the presence of 45% α-helix, 43% β-sheet, and 12% remaining structures. The α-helix content was highest at pH 7.0, where glucoamylase is optimally active. This observation points towards the possible $(\alpha/\alpha)_6$ barrel catalytic domain in TGA, as reported in microbial glucoamylases. Thermal denaturation curves of the pure protein at different pH values revealed maximum stability at pH 7.0, where no change in the secondary structure was observed upon heating in the temperature range between 20 °C and 60 °C. The observed midpoint of thermal denaturation (T_m) of glucoamylase at pH 7.0 was 67.1 °C, which decreased on either sides of this pH. Thermostability of TGA enhanced in the presence of starch (0.1%) as no transition curve was obtained in the temperature range between 20 °C and 85 °C. The only product of TGA action on starch was glucose, and it did not exhibit transglycosylation activity even at 40% glucose that can also be considered as an advantage during starch saccharification.

Keywords Glucoamylase · *Thermomucor indicae-seudaticae* · Circular dichroism · Heat denaturation · Transglycosylation

P. Kumar · T. Satyanarayana (✉)
Department of Microbiology, University of Delhi South Campus, Benito Juarez Road,
New Delhi 110 021, India
e-mail: tsnarayana@gmail.com

A. Islam · F. Ahmad
Centre for Interdisciplinary Research in Basic Sciences, Jamia Millia Islamia, Jamia Nagar,
New Delhi 110 025, India

Abbreviations

TGA	*Thermomucor indicae-seudaticae* glucoamylase
T_m	midpoint of thermal denaturation
CD	circular dichroism
f_α, f_β, f_t and f_r	fractions of α-helix, β-sheet, β-turn, and random coil, respectively
f_D	fraction of denatured protein

Introduction

Glucoamylase (E.C. 3.2.1.3, α-1,4; 1,6-glucoglucano hydrolase) is one of the widely exploited biocatalysts in the food industry. It catalyzes the sequential cleavage of α-1,4 glycosidic bonds from the non-reducing ends of starch and related oligo- and poly-saccharides, while slowly hydrolyzing α-1,6 linkages, to yield β-D-glucose [1]. The commercial potential of glucoamylase lies in its ability to saccharify partially hydrolyzed starch (dextrin) to yield glucose as the major end product, which is an important substrate for a number of food and fermentation industries involved in the production of ethanol, amino acids, organic acids, and high glucose and fructose syrups, etc. [2, 3].

The enzymatic starch hydrolysis is typically a multi-enzyme process that requires synergistic action of glucoamylase and other endo- and exo-amylases. Hence, the synchronization among participating enzymes becomes a crucial factor and those sharing common pH and temperature optima for the catalysis could prove advantageous in formulating a simpler and more economical process for starch hydrolysis [4]. The acidic pH optimum (pH 4.5–5.0) of currently used glucoamylase from *Aspergillus* spp. adds an additional step of pH adjustment during saccharification that seriously affects its performance and increases the process costs [5, 6]. A glucoamylase with optimal activity in the neutral pH range could greatly simplify the process, and hence, directed mutagenesis to improve pH performance of the commercially used glucoamylase has been the obvious research area over the years [7]. However, only modest success has been achieved until now with a mutant enzyme showing 0.4 units higher pH optimum [8]. In this regard, the structural analysis of enzymes naturally active around neutral pH could be useful in designing more productive mutations. A number of studies have been carried out to understand the structure and protein engineering of glucoamylase from *Aspergillus* spp. [6–12]. There is hardly any information available on the secondary or tertiary structures of glucoamylases optimally active around neutral pH, although the primary structures of some of these enzymes have been determined [13, 14].

We have earlier reported a unique glucoamylase from the thermophilic mold *Thermomucor indicae-seudaticae* that shows optimal activity around neutral pH, and proposed an ideal process for starch saccharification using α-amylase and amylopullulanase from two different strains of *Geobacillus thermoleovorans* [15, 16]. In this investigation, we have attempted to elucidate the secondary structure of glucoamylase from *T. indicae-seudaticae* (TGA) using CD spectroscopy and correlated the changes in its structure and thermal stability with catalytic activity. The important structural and functional features of the enzyme are being reported.

Materials and Methods

Source of Culture

The thermophilic mold *T. indicae-seudaticae* (CBS 104.75) was isolated by Subrahmanyam et al. from a compost sample from Pune, India [17]. *T. indicae-seudaticae* was routinely

grown on Emerson's YpSs agar (g l^{-1}: starch 20, yeast extract 4, K_2HPO_4 1, $MgSO_4$ 0.5, agar 20, pH 7.0) at 40 °C [18]. The culture was stored at 4 °C and also preserved in glycerol at −20 °C. The glucoamylase production was carried out in submerged fermentation [19].

Purification of Glucoamylase

TGA was purified by conventional anion exchange and gel filtration chromatographic techniques using AKTA FPLC system (Amersham Biosciences Inc., Piscataway, USA). The different solutions and buffers used during purification were filtered through 0.22-μm filters and degassed before use. All steps of purification were performed in a temperature-controlled chamber at 25 °C. The crude culture filtrate was concentrated by acetone precipitation (80% saturation). The precipitate was resuspended in sodium phosphate buffer (50 mM, pH 7.0) and dialyzed against the same buffer. The protein sample was loaded on a pre-packed 'Resource Q' anion exchange column (equilibrated with pH 7.0 phosphate buffer) and eluted using NaCl gradient (0.1 to 1.0 M in pH 7.0 buffer) at a flow rate of 1 ml/min. The protein peak corresponding to glucoamylase activity was collected and concentrated by Speed Vac (Centrifugal Evaporator CVE-2000, Eyela, Tokyo Rikakikai Co. Ltd.). The concentrated sample was subjected to size exclusion chromatography using a pre-packed 'HiPrep 16/60 Sephacryl S-200' High Resolution Column at a flow rate of 0.5 ml/min. Phosphate buffer (50 mM, pH 7.0) containing 150 mM NaCl was used as a mobile phase. Various fractions were collected and assayed for glucoamylase. The fractions showing glucoamylase activity were pooled and dialyzed.

The Purity of Glucoamylase and Molecular Weight Determination

The purity and nature of the protein were confirmed by performing the native and denaturing (SDS-PAGE) gel electrophoresis using 12% polyacrylamide. The purified fraction collected after size exclusion chromatography was also run on Reverse-Phase HPLC C18 column (Phenomenex, C18, 5 μ 1.D. 250×4.6 nm) to confirm the purity of glucoamylase before structural studies. The RP-HPLC analysis (detector: 280 nm) was carried out using acetonitrile (0.1% TFA):water (0.1% TFA) as solvent and reverse-phase stepwise gradient column for 0–15 min at the rate of 2% min^{-1} solvent; 15 to 45 min at 0.5% min^{-1} solvent at a flow rate of 1.0 ml min^{-1}. The molecular weight of the purified protein was determined on SDS-PAGE using medium range molecular weight markers.

Glucoamylase Assay and Protein Determination

Glucoamylase was assayed according to the study by Kumar and Satyanarayana [15]. The amount of reducing sugars liberated by the action of glucoamylase on starch was determined using dinitrosalicylic acid (DNS) reagent [20], with reference to the standard glucose. The glucoamylase activity at pH 7.0 was taken as a reference to calculate the percent activity at different pH values. The protein concentration in the enzyme samples was determined by Bradford's method using Coomassie Blue G250 [21].

End Product Analysis and Determination of Transglycosylation Activity

The identification of sugars released by the action of glucoamylase on starch was carried out by HPLC using RID-10A Shimadzu Refractive Index Detector equipped with Luna Amino Column (25 cm Phenomenex with 4.6 mm diameter) at a flow rate of 1 ml/min at

40 °C. Acetonitrile:water (3:1) was used as the solvent phase. To check whether the TGA has transglycosylation activity, glucose was used as the substrate. The enzyme was incubated with different glucose concentrations (1, 20, and 40%) under optimum conditions for glucoamylase action (pH 7.0 and 60 °C). The reaction mixtures were analyzed at regular time intervals for the condensation reactions that lead to the formation of oligosaccharides from glucose due to transglycosylation activity of glucoamylase.

N-terminal Amino Acid Sequencing and Mass Spectrometry

The purified glucoamylase was run on SDS-PAGE and electroblotted to Immobilon-P (0.45 micron) (Millipore) PVDF membrane. The N-terminal sequencing was performed by Edman degradation using 494 Procise Protein Sequencer/140C Analyzer from Applied Biosystems, Inc. at the Protein Facility, Iowa State University, USA. For LCMS studies, the appropriate protein band from the polyacrylamide gel was excised, destained, and reduced using dithiothreitol (DTT), alkylated using iodoacetamide, and digested using trypsin (Promega). The MALDI-TOF LC/MS studies were carried out using nano LCMS (Thermofinnigan LCQ Deca) at the Center for Genomic Application (TCGA), Okhla Industrial Estate, New Delhi, India.

Circular Dichroism Measurements

CD measurements were carried out in a Jasco J-715 spectropolarimeter with a Peltier-type temperature controller (PTC-348 WI). The instrument was calibrated with (+)-10-camphorsulphonic acid. The near- and far-UV CD spectra of glucoamylase were recorded in the wavelength range of 320-240 and 250-205 nm, respectively. Depending on the enzyme concentration, rectangular quartz cells with 0.1 cm and 1.0 cm path length were used. The raw CD data at a given wavelength, λ were converted into mean residue ellipticity, $[\theta]_\lambda$ (expressed in deg cm^2 dmol^{-1}) using the relation,

$$[\theta]_\lambda = \frac{\theta_\lambda M_0}{10lc} \tag{1}$$

where θ_λ is the observed ellipticity in millidegrees at wavelength λ, M_0 is the mean residue weight of the protein, c is the protein concentration (mg/cm^3), and l is the path length of the cell (cm). All protein solutions were prepared in the filtered and degassed 50 mM buffers of different pH values (HCl–KCl, pH 2; glycine–HCl, pH 4; sodium phosphate, pH 6–8; and glycine–NaOH, pH 9–12).

Estimation of Secondary Structure from the Far-UV CD Spectrum

The secondary structure in glucoamylase was estimated using the relation in which $[\theta]_\lambda^{\mathrm{P}}$ (the observed mean residue ellipticity of the protein) is related as the linear combination of all structures, i.e.,

$$[\theta]_\lambda^{\mathrm{P}} = f_\alpha[\theta]_\lambda^\alpha + f_\beta[\theta]_\lambda^\beta + f_t[\theta]_\lambda^t + f_r[\theta]_\lambda^r \tag{2}$$

where f_α, f_β, f_{t} and f_{r} are the fractions of α-helix, β-sheet, β-turn, and random coil, respectively, and $[\theta]_\lambda^\alpha$, $[\theta]_\lambda^\beta$, $[\theta]_\lambda^t$ and $[\theta]_\lambda^r$ are the mean residues ellipticities of the pure

α-helix, β-sheet, β-turn, and random coil at wavelength λ, respectively. Due to the uncertainty of $[\theta]_\lambda^t$ of proteins and inaccessibility of measurements beyond 205 nm, Eq. 2 was reduced to the following form,

$$[\theta]_\lambda^P = f_\alpha[\theta]_\lambda^\alpha + f_\beta[\theta]_\lambda^\beta + f_r[\theta]_\lambda^R \tag{3}$$

where R represents structures which are not the part of α-helix and β-sheet. Using the data provided by Yang et al. for the reference spectra [22], the various CD spectra of glucoamylase were analyzed for the elements of secondary structure according to Eq. 3.

Thermal Denaturation Measurements

Thermal denaturation studies were carried out in a Jasco J-715 spectropolarimeter equipped with a Peltier-type temperature controller (PTC-348 WI) with a heating rate of 1 °C/min. This scan rate was found to provide adequate time for equilibration. The change in CD at 222 nm of the protein solution was measured in the temperature range 20 °C to 80 °C. About 610 data points of each transition curve were collected. The reversibility of the thermal denaturation was checked by matching the CD spectra of TGA before and after the denaturation. The raw CD data were converted into $[\theta]_\lambda$, the mean residue ellipticity (deg cm^2 $dmol^{-1}$) at a given wavelength λ using Eq. 1. Assuming that the heat-induced denaturation is a two-state process, each apparent two-state, heat-induced denaturation curve at a given pH was analyzed for the fraction denatured, f_D associated with the equilibrium, native state↔denatured state, using the relation,

$$f_D = \frac{y(T) - y_i(T)}{y_F(T) - y_i(T)} \tag{4}$$

where $y(T)$ is the observed optical property at T K, and y_i (T) and y_F (T) are the optical properties of the initial and final states of the protein at T K, respectively. T_m, the midpoint of thermal denaturation, is defined as the temperature at which f_D equals 0.5. It has been observed that y_i (T) and y_F (T) are independent of temperature at each pH.

Results

Purification of Glucoamylase

Glucoamylase from *T. indicae-seudaticae* was purified using conventional ion exchange and gel filtration chromatographic techniques. A majority of the proteins from the crude culture concentrate displayed affinity towards the anion exchanger at pH 7.0. The active fractions showing glucoamylase activity eluted with 0.6 M NaCl (Fig. 1a). The protein fractions having enzyme activity were pooled, concentrated, and subjected to size exclusion chromatography (Fig. 1b). The protein peak corresponding to glucoamylase activity was collected and resolved on the native as well as denaturing PAGE. After silver staining, a single band appeared on both the native-PAGE and SDS-PAGE, which confirmed the homogeneity and monomeric nature of the protein (Fig. 1c). The molecular mass of glucoamylase on SDS-PAGE was approximately 45 kDa. The purity of the enzyme was further confirmed by reverse-phase HPLC (RP-HPLC) analysis (Fig. 1d).

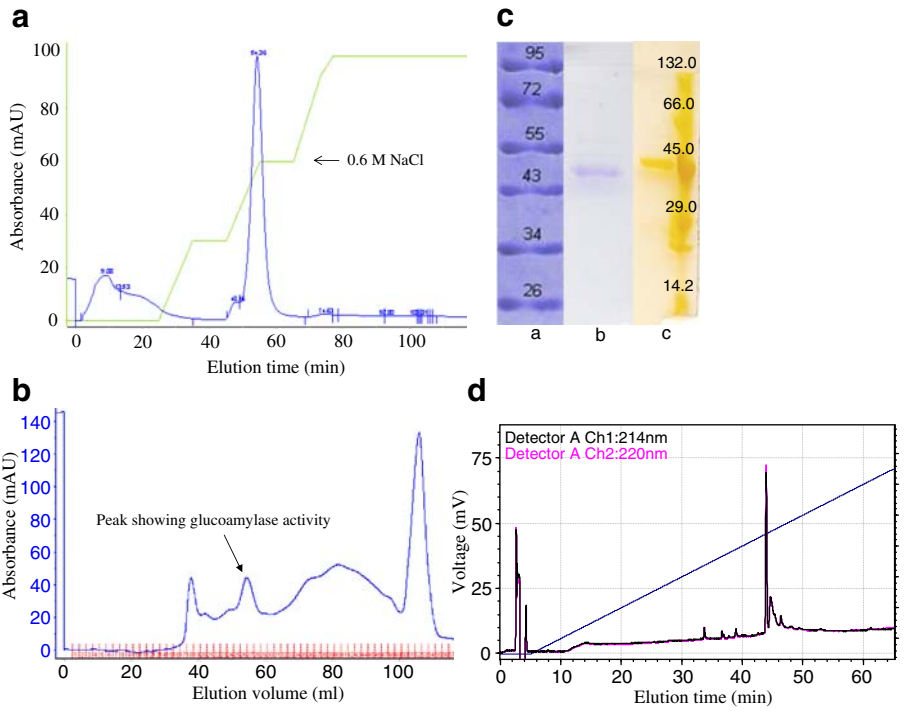

Fig. 1 **a** Elution profile of glucoamylase bound to 'Resource Q' anion exchange column. **b** Size exclusion chromatography using HiPrep Sephacryl S-200 column. **c** Gel electrophoresis of purified glucoamylase: Coomassie-stained markers (*a*), purified glucoamylase (*b*) on native-PAGE, and silver-stained purified glucoamylase with markers on SDS-PAGE (*c*). **d** Reverse-phase HPLC (RP-HPLC) analysis of the purified glucoamylase

Sequence Analysis

The sequence of ten amino acids from the N-terminus of glucoamylase was DEG TIPVTDY. Although this sequence showed less homology with glucoamylases reported from other microorganisms, significant homology was detected with a member of the family 15 glycoside hydrolase, i.e., glucoamylase from *Methylobacterium* sp. 4-46 (accession number ACA18119, www.ncbi.nlm.nih.gov/):

GTI**P**VTDY Glucoamylase from $T.\,indicae-seudaticae(TGA)$

GTI**R**VTDY Glycosidehydrolase $15-$ related $[Methylobacterium\,\text{sp.}\,4-46]$

The MALDI-TOF LC/MS analysis of the purified enzyme yielded three peptides with significant hits whose sequences were GAGLVVVSKDGR, RHETNTTGTSQPQ QHNLER, and ASCSWPGK. The N-terminal sequence of the purified glucoamylase and the peptide sequences generated by MALDI-TOF represent around 8.4% of the 45 kDa TGA.

Confirmation of the Glucoamylase Action and Transglycosylation Activity

HPLC analysis of the glucoamylase–starch reaction mixture at various time intervals revealed only one peak corresponding to the retention time of glucose (Fig. 2a–c), which confirms the

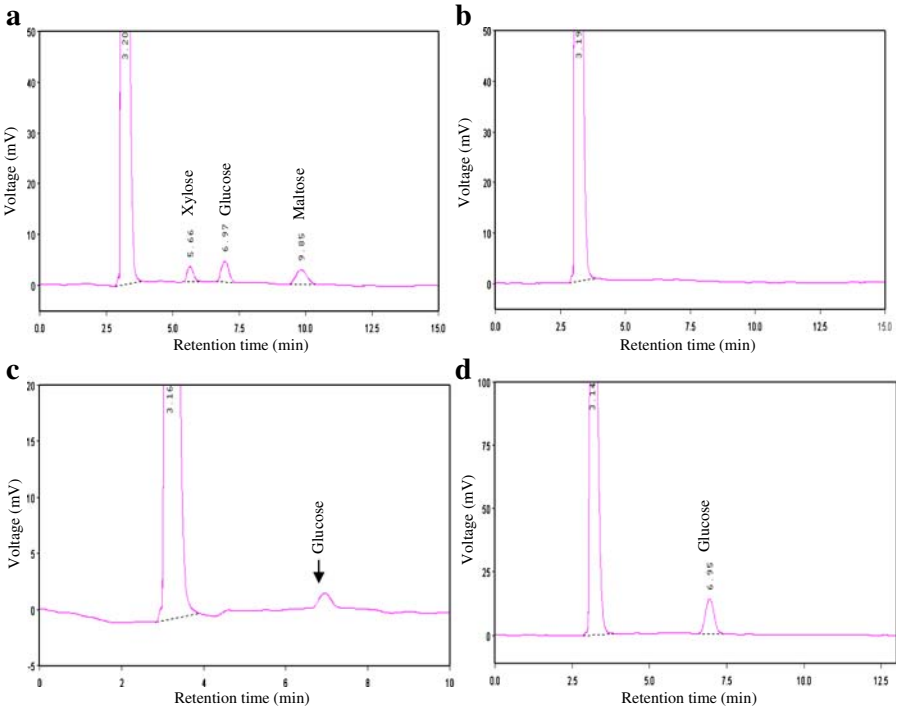

Fig. 2 HPLC profiles of xylose, glucose and maltose standards (**a**), starch (control) without glucoamylase (**b**), glucoamylase–starch reaction mixture after 1 h of incubation at 60 °C (**c**), and glucoamylase–glucose reaction mixture after 24 h of incubation at 60 °C (**d**)

enzyme to be a glucoamylase. Interestingly, glucoamylase did not show any trans-glycosylation activity on glucose even at high concentration (40%), as no extra peaks except glucose were detected up to 24 h of incubation under optimum reaction conditions (Fig. 2d).

Secondary and Tertiary Structures of TGA

Figure 3 illustrates the near-UV CD spectrum of glucoamylase showing a peak with a maximum at around 278 nm. In order to estimate the secondary structure of glucoamylase at different pH values, the far-UV CD spectra were recorded at 25 °C (Fig. 4). The measurements of CD spectra below 205 nm were not feasible due to high-tension (HT) voltage (HT voltage>600). A far-UV CD spectrum of the enzyme was also recorded at pH 7.0 and 60 °C (spectrum not shown), which was found identical to that measured at pH 7.0 and 25 °C. The $[\theta]_{222}$ value of TGA was highest at pH 7.0, which decreased on the both sides of this pH (see inset in Fig. 4). The results of the analysis of CD spectra, shown in Fig. 4, for the secondary structural elements using Eq. 3 are given in the Table 1. It should be noted that the β-turn and random coil components are summed up and presented as remaining structure, R.

Thermal Denaturation of Glucoamylase

Glucoamylase at pH values 6.0, 7.0, 9.0 and 10.0 was heated from 20 °C to 80 °C to observe changes in $[\theta]_{222}$, a measure of secondary structure index [23]. These denaturation

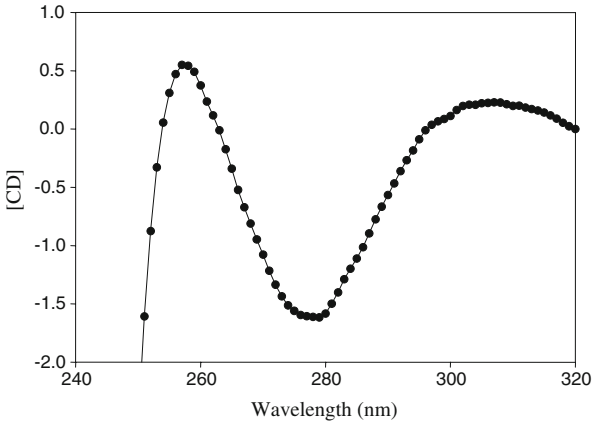

Fig. 3 The near-UV CD spectrum of glucoamylase at 25 °C and pH 7.0

curves (not shown) were analyzed for f_D as function of temperature using Eq. 4. Figure 5 shows the normalized transition curves at different pH values. The values of T_m, the temperature at which f_D=0.5, were determined from these curves, which are given in Table 1. It is seen in the inset of Fig. 4 that glucoamylase has lost most of its secondary structure at pH 2.0 and 4.0. Heating of the enzyme at these pH values did not induce further change in structure. This is the reason for not showing T_m values in the Table 1. While on the higher side of the pH, i.e., at pH 12 and above, glucoamylase precipitated on heating

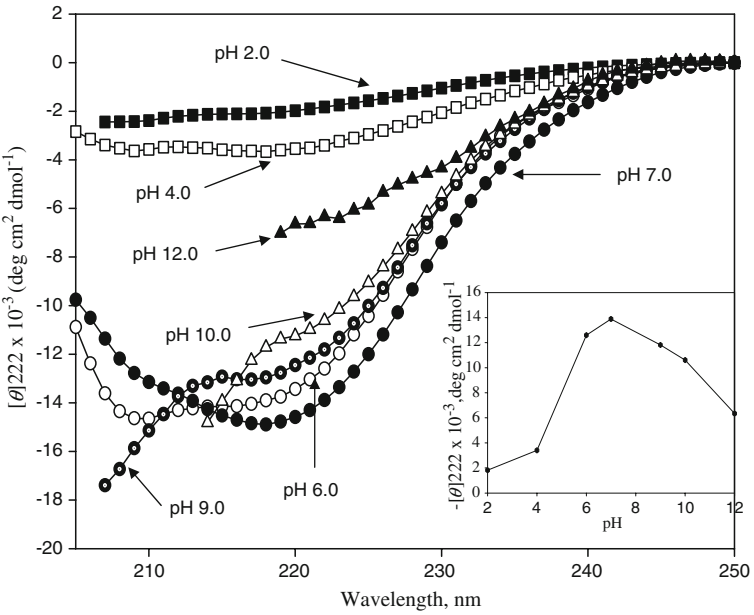

Fig. 4 The far-UV CD spectra of glucoamylase at different pH values. The inset shows the plot of $[\theta]_{222}$ versus pH

Table 1 Characteristics of glucoamylase at different pH values.

pH	$[\theta]_{222}$	α-helix (%)	β-sheet (%)	R[a] (%)	T_m(°C)
2	−1,824	0	17	83	–
4	−3,400	14	19	67	–
6	−12,595	34	38	28	65.6±0.1
7	−13,889	45	43	12	67.1±0.2
9	−11,809	41	48	11	65.5±0.1
10	−10,613	39	50	11	63.3±0.1
12	−6,339	30	17	53	–[b]

[a] R represents remaining structures, which are not the part of α-helix and β-sheet

[b] There was visible irreversible aggregation of the protein upon heating at pH 12.0

and hence, it was not possible to calculate T_m. As the pH was increased or decreased from 7.0, the T_m values decreased (Table 1). The thermal denaturation of glucoamylase in the presence of its substrate (starch) showed no transition even on heating up to 85 °C (data not shown), suggesting that the enzyme is stabilized by the substrate against heat denaturation and is more stable under process conditions.

Function Studies

The catalytic activity of glucoamylase was measured at different pH values. Figure 6 shows a plot of percent glucoamylase activity versus pH. This figure also depicts the plots of f_α, f_β and T_m versus pH to present a correlation between secondary structure, stability and catalytic activity of TGA as a function of pH. Maximum glucoamylase activity was recorded at pH 7.0 that decreased on either sides of this pH. Similarly, TGA exhibited highest α-helix content and T_m at pH 7.0, indicating the protein to be maximally stable at this pH.

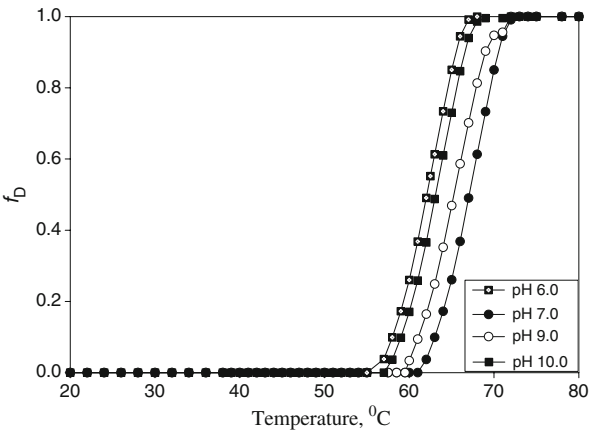

Fig. 5 The normalized thermal denaturation profiles of amylase at different pH values (f_D is the fraction of the enzyme in the denatured state and is defined in the "Materials and Methods" section)

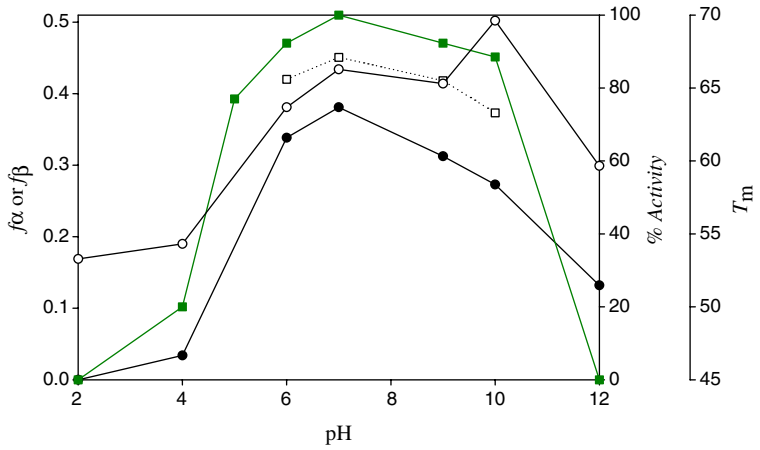

Fig. 6 Structure–function relationship of glucoamylase as a function of pH. Fractions f_α (*filled circle*) and f_β (*empty circle*) are plotted on the *left axis* while the percent activity (*filled circle*) is plotted on the *right axis*. The midpoint of thermal denaturation, T_m, (*empty square*), is plotted on the additional *right axis*

Discussion

Glucoamylase from the thermophilic mold *T. indicae-seudaticae* exhibits optimal activity at neutral pH, a rare feature among microbial glucoamylases that is expected to offer potential advantages during starch processing [15, 16]. In order to understand the rationale for optimum catalytic activity of TGA at neutral pH, the secondary structure of this unique glucoamylase was studied using circular dichroism spectroscopy as a function of pH to establish structure–function relationship. To get reliable structural data from CD, the protein must have high degree of purity. The purified glucoamylase from *T. indicae-seudaticae* used for structural studies appeared as a homogeneous protein band of around 45 kDa on SDS-PAGE. The elution profile of TGA on C_{18} reverse-phase column confirmed the purity of the protein.

The N-terminal amino acid sequence of TGA displayed significant homology with a bacterial glucoamylase from *Methylobacterium* sp. 4-46. However, it appeared to be distantly related to fungal/yeast glucoamylases that could possibly have a role in maintaining enzyme activity at higher pH. A serious problem with most glucoamylases is their transglycosylation activity that leads to the accumulation of maltose, isomaltose, and some other oligosaccharides at the expense of glucose by catalyzing the reverse reaction to lower the final glucose yield [5, 6]. Quite interestingly, transglycosylation activity was not detected in TGA on its incubation with 40% glucose under optimum reaction conditions up to 24 h.

The near-UV CD spectrum of glucoamylase at pH 7.0 and 25 °C showed the enzyme to contain a good amount of tertiary structure (Fig. 3). The near-UV CD spectrum of proteins is due to the tight packing of side chains of aromatic amino acids and disulfide bonds [24]. TGA showed a peak around 278 nm, which is, most probably, due to the buried asymmetric tyrosine and tryptophan residues. It is noteworthy that the structural studies of other microbial glucoamylases have revealed the involvement of a number of buried tyrosine residues in substrate binding and catalysis [25–28].

Analysis of the far-UV CD spectra of TGA shows that the elements of secondary structure are sensitive to the pH of the medium (see Table 1). TGA contained 45% α-helix

and 43% β-structure at pH 7.0. The far-UV CD measurements of glucoamylases from other fungi at their optimal pH have shown the presence of 30–35% α-helix, 24–36% β-structure, and the rest, aperiodic structures [29]. The crystal structure determinations (http://www.rcsb.org/pdb) had also revealed a very high content of α-helix in *Aspergillus awamori* (48%) and *Saccharomycopsis fibuligera* (51%) glucoamylases.

The maximum T_m for TGA, 67.1 °C was observed at pH 7.0, which is quite close to the maximum T_m of the well-characterized *Aspergillus niger* glucoamylase (69.7 °C). As observed in the core of the enzyme from *T. indicae-seudaticae*, T_m of *Aspergillus* glucoamylase was at a maximum at pH 5.0 where the latter exhibited maximum catalytic activity [30]. Besides native stability, it is equally important to understand the stability of an enzyme in the presence of substrate to assess its operational stability under enzyme-substrate reaction conditions. Hence, thermal denaturation of glucoamylase was carried out in the presence of its substrate (0.1% starch) at pH 7.0. Starch stabilized the protein against temperature denaturation and increased its melting temperature above 85 °C (data not shown). Thus, as in other enzymes, substrate affords stability to glucoamylase [31]. It is noteworthy that the wild-type and the hyperthermostable mutants of *Bacillus licheniformis* α-amylase were substantially stable in the presence of starch [32]. The stabilizing effect of starch could be due to the non-covalent interactions with the enzyme that protect the protein against denaturation [32]. The protective nature of starch has also been suggested against chemical denaturation of *Geobacillus thermoleovorans* α-amylase by guanidinium chloride [33].

The plots of elements of secondary structure, stability and catalytic activity of TGA versus pH showed that f_α, T_m, and enzymatic activity of glucoamylase are maximum at pH 7.0, which decreased on either side of this pH (Fig. 6). Glucoamylase activity data and changes in α-helical structure against pH denaturation strongly correlate with T_m of the protein, which is the index of protein stability. This structure–function correlation data highlights that the maintenance of appropriate α-helical structure is critical in retaining the activity in glucoamylase and hints towards the typical $(\alpha/\alpha)_6$ barrel active site reported in microbial glucoamylases [9]. On the contrary, f_β was at a maximum at pH 10.0, and it decreased on either side of this pH suggesting that β-sheet is not important for catalytic function. It is noteworthy that in fungal glucoamylases, β-sheet structure forms the starch-binding domain that does not itself catalyze starch hydrolysis but facilitate catalytic domain by binding to and disrupting the granular starch [34, 35].

Conclusions

The structural analysis of glucoamylase revealed maximum stability at pH 7.0 and 60 °C. These findings strongly corroborate with the optimum activity of glucoamylase under similar reaction conditions. However, a complete nucleotide sequence of the glucoamylase encoding gene from *T. indicae-seudaticae* would help in better understanding this thermostable and neutral enzyme, and would permit its comparison with the existing structures for related proteins. The cloning of *T. indicae-seudaticae* glucoamylase is in progress, and a part of the gene has already been cloned (data not published).

Acknowledgments PK is grateful to the Council of Scientific and Industrial Research, Government of India, for Junior/Senior Research Fellowship during the course of this investigation. This work was partially supported by the research grants from the Council of Scientific & Industrial Research and Department of Science and Technology, Government of India.

References

1. Pazur, J. H., & Ando, T. (1960). *The Journal of Biological Chemistry, 235*, 297–302.
2. Polakovic, M., & Bryjak, J. (2004). *Biochemical Engineering Journal, 18*, 57–64. doi:10.1016/S1369-703X(03)00164-5.
3. Crabb, W. D., & Shetty, J. K. (1999). *Current Opinion in Microbiology, 2*, 252–256. doi:10.1016/S1369-5274(99)80044-7.
4. Crabb, W. D. (1997). *Trends in Biotechnology, 15*, 349–352. doi:10.1016/S0167-7799(97)01082-2.
5. Ford, C. (1999). *Current Opinion in Biotechnology, 10*, 352–357. doi:10.1016/S0958-1669(99)80064-0.
6. Reilly, P. J. (1999). *Starch/Starke, 51*, 269–274.
7. Bakir, U., Coutinho, P. M., Sullivan, P. A., Ford, C., & Reilly, P. J. (1993). *Protein Engineering, 6*, 939–946. doi:10.1093/protein/6.8.939.
8. Fang, T. Y., & Ford, C. (1998). *Protein Engineering, 11*, 383–388. doi:10.1093/protein/11.5.383.
9. Aleshin, A. E., Golubev, A., Firsov, L. M., & Honzatko, R. B. (1992). *The Journal of Biological Chemistry, 267*, 19291–19298.
10. Aleshin, A. E., Firsov, L. M., & Honzatko, R. B. (1994). *The Journal of Biological Chemistry, 269*, 15631–15639.
11. Sauer, J., Sigurskjold, B. W., Christensen, U., Frandsen, T. P., Mirgorodskaya, E., Harrison, M., et al. (2000). *Biochimica et Biophysica Acta, 1543*, 275–293.
12. Jafari-Aghdam, J., Khajeh, K., Ranjbar, B., & Nemat-Gorgani, M. (2005). *Biochimica et Biophysica Acta, 1750*, 61–68.
13. Kim, M. S., Park, J. T., Kim, Y. W., Lee, H. S., Nyawira, R., Shin, H. S., et al. (2004). *Applied and Environmental Microbiology, 70*, 3933–3940. doi:10.1128/AEM.70.7.3933-3940.2004.
14. James, J. A., Robert, N., & Lee, B. H. (1996). *Biotechnology Letters, 18*, 1407–1412. doi:10.1007/BF00129344.
15. Kumar, S., & Satyanarayana, T. (2003). *Biotechnology Progress, 19*, 936–944. doi:10.1021/bp034012a.
16. Satyanarayana, T., Noorwez, S. M., Kumar, S., Rao, J. L. U. M., Ezhilvannan, M., & Kaur, P. (2004). *Biochemical Society Transactions, 32*, 276–279. doi:10.1042/BST0320276.
17. Subrahmanyam, A., Mehrotra, B. S., & Thirumalchar, M. J. (1977). *Georgia Journal of Science, 35*, 106.
18. Emerson, R. (1941). *Lloydia, 4*, 77–144.
19. Kumar, P., & Satyanarayana, T. (2007). *Bioresource Technology, 98*, 1252–1259. doi:10.1016/j.biortech.2006.05.019.
20. Miller, G. L. (1959). *Analytical Chemistry, 31*, 426–428. doi:10.1021/ac60147a030.
21. Bradford, M. M. (1976). *Analytical Biochemistry, 72*, 248–254. doi:10.1016/0003-2697(76)90527-3.
22. Yang, J. T., Wu, C. S., & Martinez, H. M. (1986). *Methods in Enzymology, 130*, 208–271. doi:10.1016/0076-6879(86)30013-2.
23. Ahmad, F., & Bigelow, C. C. (1990). *Biopolymers, 29*, 1593–1598. doi:10.1002/bip.360291209.
24. Schmid, F.X. (1997). In T.E. Creighton (Ed.), *Protein structure: A practical approach* pp. 261-297. Oxford University Press.
25. Christensen, T., Frandsen, T. P., Kaarsholm, N. C., Svensson, B., & Sigurskjold, B. W. (2002). *Biochimica et Biophysica Acta, 1601*, 163–171.
26. Svensson, B., & Sierks, M. R. (1992). *Carbohydrate Research, 227*, 29–44. doi:10.1016/0008-6215(92)85059-9.
27. Clarke, A. J., & Svensson, B. (1984). *Carlsberg Research Communications, 49*, 559–566. doi:10.1007/BF02908684.
28. Chou, W. I., Pai, T. W., Liu, S. H., Hsiung, B. K., & Chang, M. D. T. (2006). *The Biochemical Journal, 396*, 469–477. doi:10.1042/BJ20051982.
29. Shenoy, B. C., Katwa, L. C., Appu Rao, A. G., & Raghavendra Rao, M. R. (1985). *Journal of Biosciences, 7*, 399–419. doi:10.1007/BF02716801.
30. Wang, C., Eufemi, M., Turano, C., & Giartosio, A. (1996). *Biochemistry, 35*, 7299–7307. doi:10.1021/bi9517704.
31. Pace, C. N., & McGrath, T. (1980). *Biological Chemistry, 255*, 3862–3865.
32. Declerck, N., Machius, M., Chambert, R., Wiegand, G., Huber, R., & Gaillardin, C. (1997). *Protein Engineering, 10*, 541–549. doi:10.1093/protein/10.5.541.
33. Uma Maheswar Rao, J. L., & Satyanarayana, T. (2008). *Applied Biochemistry and Biotechnology, 150*, 205–219. doi:10.1007/s12010-008-8171-x.
34. Sorimachi, K., Jacks, A. J., Le Gal-Coeffet, M. F., Williamson, G., & Archer, D. B. (1996). *Journal of Molecular Biology, 259*, 970–987. doi:10.1006/jmbi.1996.0374.
35. Southall, S. M., Simpson, P. J., Gilbert, H. J., Williamson, G., & Williamson, M. P. (1999). *FEBS Letters, 447*, 58–60. doi:10.1016/S0014-5793(99)00263-X.